MITSUBISHI ELECTRIC RESEARCH LABORATORIES
https://www.merl.com

Induction Machines for Precision Positioning: Part I - Parameter Estimation

Zhao, Qianhong; Wang, Yebin; Sato, Go; Fujita, Tomoya

TR2026-168 November 04, 2026

Abstract

This paper investigates parameter estimation of an induction machine (IM) for torque bound construction, which is essential for trajectory planning and control in precision positioning systems. The problem differs from the well-studied one in speed-sensorless drives: speed measurement is available and all parameters in the IM model are treated as unknown. To this end, we first determine the subset of parameters required to construct torque bound, thereby avoid estimating all parameters. Then a flux-free representation of the IM model is derived to facilitate parameter estimation based on voltages, currents, and speed measurements. With the flux-free model established, a dynamic regressor extension and mixing based adaptive law is employed to ensure convergent estimation of the subset of parameters, under a less restrictive persistent excitation condition. Simulation validates the effectiveness of the proposed scheme.

World Congress of the International Federation of Automatic Control (IFAC) 2026

© 2026Licensed under the Creative Commons BY-NC-ND 4.0 license http://creativecommons.org/licenses/by-nc-nd/4.0/.

Mitsubishi Electric Research Laboratories, Inc.
201 Broadway, Cambridge, Massachusetts 02139

Induction Machines for Precision Positioning: Part I - Parameter Estimation

Qianhong Zhao * **Yebin Wang** ** **Go Sato** *** **Tomoya Fujita** ***

* *Department of Electrical and Computer Engineering, University of Virginia, Charlottesville, VA 22903, USA (e-mail: qz2nv@virginia.edu)*
** *Mitsubishi Electric Research Laboratories (MERL), Cambridge, MA 02139, USA (e-mail: yebinwang@ieee.org)*
*** *Mitsubishi Electric Advanced R&D Center, Amagasaki, Japan, (e-mail: {Sato.Go@dh.MitsubishiElectric.co.jp, Fujita.Tomoya@ay.mitsubishielectric.co.jp})*

Abstract: This paper investigates parameter estimation of an induction machine (IM) for torque bound construction, which is essential for trajectory planning and control in precision positioning systems. The problem differs from the well-studied one in speed-sensorless drives: speed measurement is available and all parameters in the IM model are treated as unknown. To this end, we first determine the subset of parameters required to construct torque bound, thereby avoid estimating all parameters. Then a flux-free representation of the IM model is derived to facilitate parameter estimation based on voltages, currents, and speed measurements. With the flux-free model established, a dynamic regressor extension and mixing based adaptive law is employed to ensure convergent estimation of the subset of parameters, under a less restrictive persistent excitation condition. Simulation validates the effectiveness of the proposed scheme.

Keywords: Induction machine, adaptive estimation

1. INTRODUCTION

Induction machines (IMs) are widely used in variable speed applications for rugged construction, cost-effectiveness, compact design, and low maintenance requirements Leonhard (2001). Its adoption for precision positioning, where the knowledge of motor torque bound plays a crucial role in system performance, is however limited.

In order to construct the torque bound of the IM, one must know the dynamic model parameters. Similar to work Lu et al. (2024), the torque bound reconstruction for the IM entails to solve the more challenging state and parameter estimation problem, which have attracted a lot of attention, for example Ansuj et al. (1989); Reddy et al. (2022); Wang et al. (2020); You et al. (2018); Travieso-Torres et al. (2024). For the case that only stator currents are measured, extensive research have focused on estimating the speed or position of the shaft and the fluxes to facilitate speed-sensorless vector control at the current control level, to name a few, Luenberger observer Hinkkanen (2004); You et al. (2018); Qu et al. (2014), adaptive observer Wang et al. (2020), extended Kalman filter Zerdali (2018), moving horizon estimation Zhou and Wang (2016), sliding mode observer Zaky et al. (2018), signal injection Holtz (2006); Wu et al. (2025), etc. The estimation problem tackled in this work differs from the aforementioned work in three ways: 1) both the stator currents and speed are measured; 2) all the model parameters are treated as unknown parameters; and 3) the objective of the estimation is to reconstruct torque bound to facilitate high performance precision motion control. To address this problem, it is advantageous to estimate a portion of unknown parameters required to compute torque bounds, while imposing mild conditions to ensure parameter convergence. When the full system state is measurable, all uncertain parameters of a multi-input multi-output state–space model can be estimated using the system identifiers proposed in Tao (2003) and Ioannou and Sun (1996). In contrast, when only partial system states are measurable, existing works such as Zhang (2002) and Wang et al. (2020) have demonstrated that adaptive observer techniques can still achieve parameter convergence, provided that the persistence of excitation (PE) condition is satisfied. The PE condition typically requires the system inputs to contain sufficiently rich frequency components (Tao, 2003; Ioannou and Sun, 1996), which is somewhat restrictive.

This paper focuses on parameter estimation that achieves parameter convergence under less restriction on system inputs. To avoid the practical difficulty of enforcing input signals of IM with rich and diverse frequencies to satisfy the PE condition, we adopt a dynamic regressor extension and mixing (DREM) based adaptive law introduced in Aranovskiy et al. (2017) that imposes a weaker condition, yet still guarantees parameter convergence performance.

2. PROBLEM STATEMENT

In precision positioning applications, the IM is treated as a torque actuator to drive an inertial load where its control unit (inverter) receives either velocity or position reference

⋆ This work was done while Q. H. Zhao was a research intern at MERL, Cambridge, MA 02139, USA.

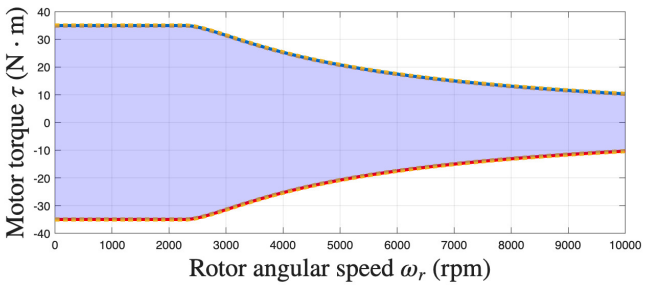

Fig. 1. Torque bounds with respect to rotor electrical angular speed ω_r: $\tau_{\min}(\omega_r)$ - red dash line, $\tau_{\max}(\omega_r)$ - blue dash line, torque capacity set $[\tau_{\min}(\omega_r), \tau_{\max}(\omega_r)]$ - light blue area.

Table 1. Notations

Notation	Description
$\lambda_{ds}, \lambda_{qs}$	stator fluxes in d- and q-axis
$\lambda_{dr}, \lambda_{qr}$	rotor fluxes in d- and q-axis
i_{ds}, i_{qs}	stator currents in d- and q-axis
v_{ds}, v_{qs}	stator voltages in d- and q-axis
ω	rotor angular speed
ω_0	angular speed of a rotating frame
ω_s	synchronous stator electrical speed
ω_r	rotor electrical angular speed
ω_{slip}	slip angular speed
T_e	torque produced by the motor
T_l	load torque
p	number of pole pairs
R_s, R_r	stator and rotor resistances
L_s, L_m, L_r	stator, mutual, and rotor inductances
σ	leakage factor, $\frac{L_s L_r - L_m^2}{L_s L_r}$
α	R_r / L_r
β	$L_m / L_r \times 1/(L_s \sigma)$
γ	$R_s/(L_s\sigma) + \alpha\beta L_m$
J	rotor inertia

trajectory. We will clarify our research problem after introducing the dynamic models of positioning systems.

2.1 System Modeling

Load positioning model The dynamic model of the load is given by

$$\begin{aligned} \dot{x} &= v \\ \dot{v} &= -\mu_v v - \mu_c \text{sgn}(v) + bu, \end{aligned} \tag{1}$$

where $x \in \mathbb{R}, v \in \mathbb{R}$ are the load position and velocity, respectively, $u \in \mathbb{R}$ is control torque in Nm, μ_v and μ_c are viscous and Coulomb friction coefficients, respectively.

System (1) is subject to a velocity-dependent control constraint: $\tau_{\min}(v) \le u \le \tau_{\max}(v)$. Fig. 1 shows an example of the motor's torque capacity. Thus, we should take into account the torque capacity of the IM while designing the control algorithm for load positioning.

IM models Table 1 lists all the notations of states and parameters in IM models.

In a reference frame rotating at speed ω_0, the IM model, under linear inductance assumption, the IM model admits the following state space representation:

$$\begin{aligned} \dot{i}_{ds} &= -\gamma i_{ds} + \omega_0 i_{qs} + \beta(\alpha\lambda_{dr} + \omega_r \lambda_{qr}) + \frac{v_{ds}}{L_s\sigma} \\ \dot{i}_{qs} &= -\omega_0 i_{ds} - \gamma i_{qs} + \beta(\alpha\lambda_{qr} - \omega_r \lambda_{dr}) + \frac{v_{qs}}{L_s\sigma} \\ \dot{\lambda}_{dr} &= -\alpha\lambda_{dr} + (\omega_0 - \omega_r)\lambda_{qr} + \alpha L_m i_{ds} \\ \dot{\lambda}_{qr} &= -\alpha\lambda_{qr} - (\omega_0 - \omega_r)\lambda_{dr} + \alpha L_m i_{qs} \\ \dot{\omega}_r &= \frac{p}{J}\left(\frac{3pL_m}{2L_r}(\lambda_{dr} i_{qs} - \lambda_{qr} i_{ds}) - T_l\right) \\ \boldsymbol{y} &= [i_{ds} \ i_{qs} \ \omega_r]^\top. \end{aligned} \tag{2}$$

The IM states are subject to operation constraints:

$$\begin{cases} i_{ds}^2 + i_{qs}^2 \le I_{\max}^2, \\ v_{ds}^2 + v_{qs}^2 \le V_{\max}^2, \end{cases} \tag{3}$$

where $I_{\max}$ and $V_{\max}$ denote the known maximum current and voltage, respectively. More details on motor modeling can be found in Leonhard (2001).

Torque capacity We use the IM model in the rotor flux-oriented frame, also named after the *dq* frame, to construct torque capacity. The angular speed ω_0 of the *dq* frame reaches the synchronous stator electrical speed ω_s which is solved from $\dot{\lambda}_{qr} = \lambda_{qr} = 0$ as $\omega_s = \omega_r + \omega_{\text{slip}}$ where $\omega_{\text{slip}} = \frac{\alpha L_m i_{qs}}{\lambda_{dr}}$ is the slip speed. The IM model in the *dq* frame is given by

$$\begin{aligned} \dot{i}_{ds} &= -\gamma i_{ds} + \omega_s i_{qs} + \beta\alpha\lambda_{dr} + \frac{v_{ds}}{L_s\sigma} \\ \dot{i}_{qs} &= -\omega_s i_{ds} - \gamma i_{qs} - \beta\omega_r\lambda_{dr} + \frac{v_{qs}}{L_s\sigma} \\ \dot{\lambda}_{dr} &= -\alpha\lambda_{dr} + \alpha L_m i_{ds} \\ \dot{\omega}_r &= \frac{p}{J}(T_e - T_l), \end{aligned} \tag{4}$$

where $T_e = \frac{3pL_m}{2L_r}\lambda_{dr} i_{qs}$. The lower bound $\tau_{\min}$ and upper bound $\tau_{\max}$ of the motor torque are computed from two programming problems subject to the steady-state condition and operation constraints (3), i.e.,

$$\begin{cases} \tau_{\max}(\omega_r) = \mathbf{max}_{i_{ds}, i_{qs}} \ \dfrac{3pL_m}{2L_r}\lambda_{dr} i_{qs} \\ \tau_{\min}(\omega_r) = \mathbf{min}_{i_{ds}, i_{qs}} \ \dfrac{3pL_m}{2L_r}\lambda_{dr} i_{qs} \end{cases}$$

subject to (3) and

$$[\dot{i}_{ds}, \dot{i}_{qs}, \dot{\lambda}_{dr}]^\top = 0. \tag{5}$$

Both $\tau_{\min}$ and $\tau_{\max}$ depend on angular speed ω_r. Note that $\tau_{\max}(\omega_r) = -\tau_{\min}(\omega_r)$.

2.2 Research Problems

We consider the control architecture as shown in Fig. 2. A parameter estimator resolves unknown parameters, whereas the torque capacity generator reconstructs the precise torque bounds. The motion planner computes a dynamically feasible reference $x^*(t)$ without violating the torque bounds, while the tracking controller ensures the load position x follows x^* accurately.

We focus on convergent parameter estimation with measurements i_{ds}, i_{qs}, v_{ds}, v_{qs}, and ω_r. We first identify the necessary parameters required for torque bound construction; and then design a convergent parameter estimation algorithm to identify the values of unknown parameters. Accordingly, this paper will solve two major problems:

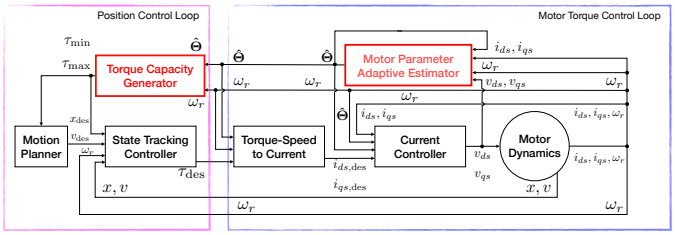

Fig. 2. The closed-loop planning and control system.

Problem 2.1. *Given the IM model* (4) *and the available measurements of* p, i_{ds}, i_{qs}, *and* ω_r, *identify the set of parameters* $\boldsymbol{\Theta}$ *that must be estimated in order to solve the optimization problem* (5)

Problem 2.2. *Given the IM models* (2) *and* (4) *with measurements of rotor electrical angular speed* ω_r, *currents* i_{ds} *and* i_{qs}, *and voltages* v_{ds} *and* v_{qs}, *construct the parameter estimation scheme for estimating all the necessary parameters* $\boldsymbol{\Theta}$ *identified by solving Problem 2.1.*

2.3 Technical Issues of Parameter Estimation

Standard parameter estimation procedure involves two steps. The model of a linear time-invariant (LTI) systems is first reformulated as the form of

$$\mathcal{Y}(t) = \boldsymbol{\Theta}^{*\top}\boldsymbol{\Phi}(t), \tag{6}$$

where both $\mathcal{Y}(t) \in \mathbb{R}$ and the regressor $\boldsymbol{\Phi}(t) \in \mathbb{R}^n$ are measurable signals, and $\boldsymbol{\Theta}^*$ is the unknown parameter vector to be estimated. In the second step, an adaptive law is designed for the estimates $\hat{\boldsymbol{\Theta}}(t)$ of the unknown parameter $\boldsymbol{\Theta}^*$, ensuring parameter convergence, i.e.,

$$\lim_{t\to\infty}\left(\hat{\boldsymbol{\Theta}}(t) - \boldsymbol{\Theta}^*\right) = 0. \tag{7}$$

Remark 2.3. *For estimation algorithms in Tao (2003); Ioannou and Sun (1996), parameter convergence requires the PE condition for* $\boldsymbol{\Phi}(t)$, *as well as the boundedness condition* $\boldsymbol{\Phi}(t) \in \mathcal{L}^\infty$. *The PE of* $\boldsymbol{\Phi}(t)$ *depends directly on the frequency components of the system inputs. Specifically, the more unknown parameters to be estimated, the more frequency components need to be included in the input.* □

The presence of the unmeasurable fluxes, i.e., λ_{dr} and λ_{qr}, makes it difficult to apply the adaptive-control–based system identifiers in Tao (2003) and Ioannou and Sun (1996). These identifiers rely on the assumption that the full system state vector is measurable, which is not satisfied in this case. In addition, it is challenging to ensure that the system inputs (voltages v_{ds} and v_{qs}) contains sufficiently rich frequency components to satisfy the PE condition required for parameter convergence in traditional parameter estimation schemes, while simultaneously meeting the constant-angular-speed assumption Assumption 3.1.

Although the adaptive observer in Zhang (2002) are widely used in motor systems, for example, Lu et al. (2024); Wang et al. (2020) with guarantee convergence, it suffers from the requirements of strong PE and non-trivial parameter tuning. In summary, we ought to develop a solution which derives a linear representation (6) where $\boldsymbol{\Phi}(t)$ is independent from fluxes and $\boldsymbol{\Theta}^*$ contains all necessary unknown parameters for torque bound construction; and performs parameter estimation where the requirements for parameter convergence are relaxed.

3. PARAMETER ESTIMATION WITHOUT FLUX-RELATED STATE MEASUREMENT

We first identify the necessary parameters and derive a practical flux-free model of the IM for parameter estimation. Then, we design a DREM-based adaptive law using the flux-free model.

3.1 Necessary Parameters for Torque Bound Construction

By setting $[\dot{i}_{ds}, \dot{i}_{qs}, \dot{\lambda}_{dr}]^\top = 0$, we have $L_m i_{ds} = \lambda_{dr}$ and

$$\begin{aligned}(-\gamma + \alpha\beta L_m)\, i_{ds} + \Big(\omega_r + \frac{\alpha i_{qs}}{i_{ds}}\Big) i_{qs} + \frac{v_{ds}}{L_s\sigma} = 0\\ \Big(-\omega_r - \frac{\alpha i_{qs}}{i_{ds}} - \beta\omega_r L_m\Big) i_{ds} - \gamma i_{qs} + \frac{v_{qs}}{L_s\sigma} = 0.\end{aligned} \tag{8}$$

Determining the upper bound $\tau_{\max}(\omega_r)$ in (5) is equivalent to solve the following optimization problem:

$$\begin{aligned}&\mathbf{max}_{i_{ds},i_{qs}} \ \frac{3pL_m^2}{2L_r} i_{ds} i_{qs}\\ &\text{subject to: (3) and (8).}\end{aligned} \tag{9}$$

From (9), we identify the necessary parameters being: $\frac{L_m^2}{L_r}$, $-\gamma + \alpha\beta L_m$, α, $L_s\sigma$, γ, and βL_m.

3.2 Practical Flux-free Model and Parametrization

We present a practical parameterization method based on the following common assumption Wang et al. (2020):

Assumption 3.1. *The rotor speed is measured precisely and remains constant, i.e.,* $\dot{\omega}_r = 0$.

With Assumption 3.1, the motor dynamics equation (2) is reduced to an LTI system with unknown parameters, i.e.,

$$\begin{aligned}\dot{\boldsymbol{x}} &= \boldsymbol{A}\boldsymbol{x} + \boldsymbol{B}\boldsymbol{u}\\ \dot{\omega}_r &= 0\\ \boldsymbol{y} &= [i_{ds}, i_{qs}, \omega_r]^\top,\end{aligned} \tag{10}$$

where $\boldsymbol{x} = [i_{ds}, i_{qs}, \lambda_{dr}, \lambda_{qr}]^\top$, and

$$\boldsymbol{A} = \begin{bmatrix} -\gamma & 0 & \beta\alpha & \beta\omega_r \\ 0 & -\gamma & -\beta\omega_r & \beta\alpha \\ \alpha L_m & 0 & -\alpha & -\omega_r \\ 0 & \alpha L_m & \omega_r & -\alpha \end{bmatrix},\ \boldsymbol{B} = \begin{bmatrix} \frac{1}{L_s\sigma} & 0 \\ 0 & \frac{1}{L_s\sigma} \\ 0 & 0 \\ 0 & 0 \end{bmatrix}.$$

Given the representation (10), one can readily derive the flux-free model as (11) by eliminating flux variables.

System parametrization From (11), it is straightforward to rearrange the flux-free model into

$$\boldsymbol{\mathcal{Y}}(t) = \boldsymbol{\Phi}^\top(t)\boldsymbol{\Theta}^*. \tag{12}$$

where

$$\boldsymbol{\mathcal{Y}}(t) = [\mathcal{Y}_1(t), \mathcal{Y}_2(t)]^\top = \begin{bmatrix} \dot{i}_{ds} + \omega_r \dot{i}_{qs} \\ \dot{i}_{qs} - \omega_r \dot{i}_{ds} \end{bmatrix}, \tag{13}$$

$$\boldsymbol{\Phi}(t) = [\phi_1(t), \phi_2(t)] = \begin{bmatrix} i_{ds} & i_{qs} \\ \omega_r i_{qs} & -\omega_r i_{ds} \\ -\dot{i}_{ds} & -\dot{i}_{qs} \\ \dot{v}_{ds} + \omega_r v_{qs} & \dot{v}_{qs} - \omega_r v_{ds} \\ v_{ds} & v_{qs} \end{bmatrix}, \tag{14}$$

$$-(\alpha\beta L_m-\gamma)\begin{bmatrix}\alpha & \omega_r\\ -\omega_r & \alpha\end{bmatrix}\begin{bmatrix}i_{ds}\\ i_{qs}\end{bmatrix}+\begin{bmatrix}\gamma+\alpha & \omega_r\\ -\omega_r & \gamma+\alpha\end{bmatrix}\begin{bmatrix}\dot{i}_{ds}\\ \dot{i}_{qs}\end{bmatrix}+\begin{bmatrix}\ddot{i}_{ds}\\ \ddot{i}_{qs}\end{bmatrix}=\frac{1}{L_s\sigma}\left(\begin{bmatrix}\alpha & \omega_r\\ -\omega_r & \alpha\end{bmatrix}\begin{bmatrix}v_{ds}\\ v_{qs}\end{bmatrix}+\begin{bmatrix}\dot{v}_{ds}\\ \dot{v}_{qs}\end{bmatrix}\right) \tag{11}$$

and

$$\boldsymbol{\Theta^*}=\begin{bmatrix}\Theta_1^*\\ \Theta_2^*\\ \Theta_3^*\\ \Theta_4^*\\ \Theta_5^*\end{bmatrix}=\begin{bmatrix}\alpha(\alpha\beta L_m-\gamma)\\ (\alpha\beta L_m-\gamma)\\ \gamma+\alpha\\ \frac{1}{L_s\sigma}\\ \frac{\alpha}{L_s\sigma}\end{bmatrix}. \tag{15}$$

Remark 3.2. *The parameter vector $\boldsymbol{\Theta}^*$ contains enough information for construct the torque capacity. Recall that the necessary parameters or parameter combinations are $\frac{L_m^2}{L_r}$, $-\gamma+\alpha\beta L_m$, α, $L_s\sigma$, γ, and βL_m. According to the elements of $\boldsymbol{\Theta}^*$ in* (15) *and Table 1, we have*

$$\alpha=\frac{\Theta_1^*}{\Theta_2^*}=\frac{\Theta_5^*}{\Theta_4^*},\ \gamma=\Theta_3^*-\frac{\Theta_1^*}{\Theta_2^*},\ L_s\sigma=\frac{1}{\Theta_4^*}, \tag{16}$$

$\beta L_m=\frac{\Theta_2^*+\gamma}{\alpha}$ *and* $\frac{Lm^2}{Lr}=\beta L_m L_s\sigma$. □

Signal realization of the flux-free model. The parametrized model (12) involves the first- and second-order derivatives of current and voltage (e.g., $\dot{i}_{ds}$, $\dot{i}_{qs}$, $\ddot{i}_{ds}$, $\ddot{i}_{qs}$, $\dot{v}_{ds}$, and $\dot{v}_{qs}$). Since these derivatives are not directly measurable, we next explain how such unmeasurable terms can be handled. Denote a filter $G_f(s)=1/\Lambda(s)$, where $\Lambda(s)=s^2+d_1s+d_0$ is Hurwitz and d_1 and d_0 are the tuning parameters. Filtering both sides of (12), we obtain

$$\begin{bmatrix}\frac{1}{\Lambda(s)}[\dot{i}_{ds}]\\ \frac{1}{\Lambda(s)}[\ddot{i}_{qs}]\end{bmatrix}+\begin{bmatrix}\frac{\omega_r}{\Lambda(s)}[\dot{i}_{qs}]\\ \frac{-\omega_r}{\Lambda(s)}[\dot{i}_{ds}]\end{bmatrix}=$$

$$\begin{bmatrix}\frac{1}{\Lambda(s)}[i_{ds}] & \frac{1}{\Lambda(s)}[i_{qs}]\\ \frac{\omega_r}{\Lambda(s)}[i_{qs}] & -\frac{\omega_r}{\Lambda(s)}[i_{ds}]\\ \frac{-1}{\Lambda(s)}[\dot{i}_{ds}] & \frac{-1}{\Lambda(s)}[\dot{i}_{qs}]\\ \frac{1}{\Lambda(s)}[\dot{v}_{ds}]+\frac{\omega_r}{\Lambda(s)}[v_{qs}] & \frac{1}{\Lambda(s)}[\dot{v}_{qs}]+\frac{-\omega_r}{\Lambda(s)}[v_{ds}]\\ \frac{1}{\Lambda(s)}[v_{ds}] & \frac{1}{\Lambda(s)}[v_{qs}]\end{bmatrix}^\top\boldsymbol{\Theta^*}, \tag{17}$$

which could be denoted as

$$\frac{1}{\Lambda(s)}[\mathcal{Y}](t)=\frac{1}{\Lambda(s)}[\Phi]^\top(t)\boldsymbol{\Theta^*}. \tag{18}$$

The filtered first- and second-order derivatives in (17), i.e., $\frac{1}{\Lambda(s)}[\dot{i}_{ds}]$, $\frac{1}{\Lambda(s)}[\dot{i}_{qs}]$, $\frac{1}{\Lambda(s)}[\ddot{i}_{ds}]$, $\frac{1}{\Lambda(s)}[\ddot{i}_{qs}]$, $\frac{1}{\Lambda(s)}[\dot{v}_{ds}]$, and $\frac{1}{\Lambda(s)}[\dot{v}_{qs}]$, can be obtained in the followed method.

The filter $G_f(s)$ could be realized by a state space model

$$\dot{\boldsymbol{x}}_{\boldsymbol{f}}=\boldsymbol{A_f}\boldsymbol{x_f}+\boldsymbol{B_f}\nu, \tag{19}$$

where $\boldsymbol{A}_f=\begin{bmatrix}0 & 1\\ -d_0 & -d_1\end{bmatrix}$, $\boldsymbol{B}_f=\begin{bmatrix}0\\ 1\end{bmatrix}$ and $\nu\in\mathbb{R}$ is the signal that needs to be filtered. In (19), the state $x_f\in\mathbb{R}^2$ is equivalent to $\left[\frac{1}{\Lambda(s)}[\nu],\frac{1}{\Lambda(s)}[\dot{\nu}]\right]^\top$. Then, $\frac{1}{\Lambda(s)}[\ddot{\nu}]$ could be computed by $\frac{1}{\Lambda(s)}[\ddot{\nu}]=\nu-\frac{d_1}{\Lambda(s)}[\dot{\nu}]-\frac{d_1}{\Lambda(s)}[\nu]$.

With above method, the filtered first- and second-order derivatives in (17), could be obtained through replacing ν in (19) by i_{ds}, i_{qs}, v_{ds}, and v_{qs}, respectively. This means that we have $\frac{1}{\Lambda(s)}[\boldsymbol{\mathcal{Y}}](t)$ and $\frac{1}{\Lambda(s)}[\boldsymbol{\Phi}](t)$ in (17), and are now ready to study the adaptive law for $\hat{\boldsymbol{\Theta}}(t)$ to estimate $\boldsymbol{\Theta^*}$.

3.3 DREM-based Adaptive Law

We leverage the DREM design proposed in Aranovskiy et al. (2017) for parameter estimation. The first step is extending the regressor model (17) such that the dimension of the LHS of the extended regressor model is the same as the that of the parameter vector $\boldsymbol{\Theta^*}$. Specifically, we extend (17) into the extended regression model,

$$\boldsymbol{Y_e}(t)=\boldsymbol{M}(t)^\top\boldsymbol{\Theta^*}\left[\boldsymbol{m_1}(t),\boldsymbol{m_2}(t),\ldots,\boldsymbol{m_5}(t)\right]^\top\boldsymbol{\Theta^*}, \tag{20}$$

where $\boldsymbol{Y_e}(t)\in\mathbb{R}^5$ and $\boldsymbol{M}(t)\in\mathbb{R}^{5\times5}$ because $\boldsymbol{\Theta^*}\in\mathbb{R}^5$.

This extension is easy to fulfill by utilizing several different filters in (18). For example, a satisfied extended regressor model (20) could be constructed by

$$\boldsymbol{Y_e}(t)=\begin{bmatrix}\frac{1}{\Lambda_1(s)}[\mathcal{Y}_1](t)\\ \frac{1}{\Lambda_1(s)}[\mathcal{Y}_2](t)\\ \frac{1}{\Lambda_2(s)}[\mathcal{Y}_1](t)\\ \frac{1}{\Lambda_2(s)}[\mathcal{Y}_2](t)\\ \frac{1}{\Lambda_3(s)}[\mathcal{Y}_1](t)\end{bmatrix},\boldsymbol{M}(t)=\begin{bmatrix}\frac{1}{\Lambda_1(s)}[\phi_1^\top](t)\\ \frac{1}{\Lambda_1(s)}[\phi_2^\top](t)\\ \frac{1}{\Lambda_2(s)}[\phi_1^\top](t)\\ \frac{1}{\Lambda_2(s)}[\phi_2^\top](t)\\ \frac{1}{\Lambda_3(s)}[\phi_1^\top](t)\end{bmatrix}^\top, \tag{21}$$

where $\frac{1}{\Lambda_1(s)}$, $\frac{1}{\Lambda_2(s)}$, and $\frac{1}{\Lambda_3(s)}$ are three different filters with different coefficient pairs of d_1 and d_0 in $G_f(s)$.

The second step is deriving the adaptive law for the parameter estimate $\hat{\boldsymbol{\Theta}}(t)$ for $\boldsymbol{\Theta^*}$ based on the extended regressor model (20) that guarantees the parameter convergence (7).

According to Aranovskiy et al. (2017), the adaptive law for $\hat{\boldsymbol{\Theta}}(t)$ is designed as

$$\dot{\hat{\boldsymbol{\Theta}}}(t)=\boldsymbol{\Gamma}\psi(t)\left(\boldsymbol{Y}(t)-\psi(t)\hat{\boldsymbol{\Theta}}(t)\right), \tag{22}$$

where $\boldsymbol{\Gamma}=\mathrm{diag}(\gamma_1,\gamma_2,\gamma_3,\gamma_4,\gamma_5)$, $\gamma_i>0$, $i=1,\ldots,5$, $\psi(t)$ is the determinant of $\boldsymbol{M}(t)$, i.e., $\psi(t)=\det(\boldsymbol{M}(t))$, and

$$\boldsymbol{Y}(t)=\mathrm{adj}(\boldsymbol{M}^\top(t))\boldsymbol{Y_e}(t). \tag{23}$$

When $\boldsymbol{M}(t)$ is invertible, i.e., $\det(\boldsymbol{M}(t))\neq0$, we have

$$\left(\boldsymbol{M}^\top(t)\right)^{-1}=\frac{\mathrm{adj}\left(\boldsymbol{M}^\top(t)\right)}{\det\left(\boldsymbol{M}^\top(t)\right)} \tag{24}$$

according to the definitions of the adjoint matrix and the inverse matrix. Then, (23) could be rewritten as

$$\boldsymbol{Y}=\psi(t)\boldsymbol{\Theta^*}. \tag{25}$$

Given the parameter error $\tilde{\boldsymbol{\Theta}}(t)=\hat{\boldsymbol{\Theta}}(t)-\boldsymbol{\Theta^*}$, adaptive law (22) and parametrized signal $\boldsymbol{Y}(t)$ in (25) imply

$$\dot{\tilde{\boldsymbol{\Theta}}}(t)=-\boldsymbol{\Gamma}\psi^2(t)\tilde{\boldsymbol{\Theta}}(t). \tag{26}$$

Remark 3.3. *In Aranovskiy et al. (2017), the parameter convergence property* (7) *is guaranteed by ensuring that $\psi(t)$ does not belong to the $\mathcal{L}_2$ norm space, which implies the invertibility of $\boldsymbol{M}(t)$ at certain time instants, based on the dynamics of the parameter error $\tilde{\boldsymbol{\Theta}}(t)$* (26).

Remark 3.4. *The condition for parameter estimation of the adaptive law* (22) *in Remark 3.3 usually cannot be achieved during the operation of the IM. However, by*

reviewing the adaptive law in (26)*, the parameter error can be expressed as*

$$\tilde{\mathbf{\Theta}}(t) = \tilde{\mathbf{\Theta}}(0)\, \exp\big(-\mathbf{\Gamma} \int_0^t \psi^2(\tau) d\tau \big), \tag{27}$$

which implies that if voltages $v_{ds}(t)$ *and* $v_{qs}(t)$ *in* (2) *are non-vanishing sinusoidal waves, and the coefficients of the filters* $\frac{1}{\Lambda_1(s)}$, $\frac{1}{\Lambda_2(s)}$, *and* $\frac{1}{\Lambda_3(s)}$ *are chosen such that* $\mathbf{\Gamma}\psi^2(t)$ *is sufficiently large at the time instants in the early stage, the convergence of the parameter error can be guaranteed. In this case, the parameter estimation error* $\tilde{\mathbf{\Theta}}(t)$ *converges to zero prior to the convergence of* $\psi^2(t)$*.* □

4. SIMULATION STUDY

System parameters The system parameters of the IM (10) are: $p = 2$, $R_s = 0.439\,\Omega$, $R_r = 0.41\,\Omega$, $L_s = 0.0615\,\text{H}$, $L_m = 0.0601\,\text{H}$, $L_r = 0.0619\,\text{H}$, $I_{\max} = 20\,\text{A}$, and, $V_{\max} = 380\sqrt{\frac{2}{3}}\,\text{V}$. The rotor electrical angular speed is set to 188.5rad/sec, which is equivalent to 1800rpm. This is possible when the IM is driven by another motor.

The initial values of parameter estimates are set as 90 percents of the nominal values, i.e., $\hat{\mathbf{\Theta}} = 0.9\mathbf{\Theta}^*$.

System input The system input is selected as

$$\begin{aligned} v_{ds}(t) &= 8\sin(6\pi t) \\ v_{qs}(t) &= 8\cos(6\pi t). \end{aligned} \tag{28}$$

Simulation cases We consider four different simulations for different combinations of the gain, Γ, in the adaptive law (22) and the filter selections. The detailed settings of these four cases are:

- **Case I**: $\mathbf{\Gamma} = \text{diag}(30000, 30000, 30000, 30000, 30000)$, $\frac{1}{\Lambda_1(s)} = \frac{1}{s^2+3s+5}$, $\frac{1}{\Lambda_2(s)} = \frac{1}{s^2+11s+7}$, $\frac{1}{\Lambda_3(s)} = \frac{1}{s^2+17s+13}$
- **Case II**: $\mathbf{\Gamma} = \text{diag}(300, 300, 300, 300, 300)$, $\frac{1}{\Lambda_1(s)} = \frac{1}{s^2+s+0.05}$, $\frac{1}{\Lambda_2(s)} = \frac{1}{s^2+25s+0.1}$, $\frac{1}{\Lambda_3(s)} = \frac{1}{s^2+4s+0.25}$
- **Case III**: $\mathbf{\Gamma} = \text{diag}(30000, 30000, 30000, 30000, 30000)$, $\frac{1}{\Lambda_1(s)} = \frac{1}{s^2+s+0.05}$, $\frac{1}{\Lambda_2(s)} = \frac{1}{s^2+25s+0.1}$, $\frac{1}{\Lambda_3(s)} = \frac{1}{s^2+4s+0.25}$
- **Case IV**: $\mathbf{\Gamma} = \text{diag}(60000, 60000, 60000, 60000, 60000)$, $\frac{1}{\Lambda_1(s)} = \frac{1}{s^2+s+0.05}$, $\frac{1}{\Lambda_2(s)} = \frac{1}{s^2+25s+0.1}$, $\frac{1}{\Lambda_3(s)} = \frac{1}{s^2+4s+0.25}$.

Simulation results The trajectory of parameter estimation errors are shown in Fig. 3, where all the estimate errors converge within 1.5 second in Cases III and IV.

The reason why Case I fails to achieve parameter convergence can be understood by combining (27) with Fig. 4. Fig. 4 illustrates the order-of-magnitude difference of $\psi(t)$ between the two filter sets used in Cases I–IV. The vertical axis indicates how many orders of magnitude $|\psi_2(t)|$, corresponding to Cases II–IV, exceeds $|\psi_1(t)|$, which is the value used in Case I.For example, when $\log_{10} \frac{|\psi_2(t)|+\epsilon}{|\psi_1(t)|+\epsilon} = 3$, it indicates that $|\psi_2(t)|$ is approximately 10^3 times larger than $|\psi_1(t)|$. Thus, the figure clearly shows that the magnitude of $\psi_2(t)$ is significantly larger than that of $\psi_1(t)$. Using this

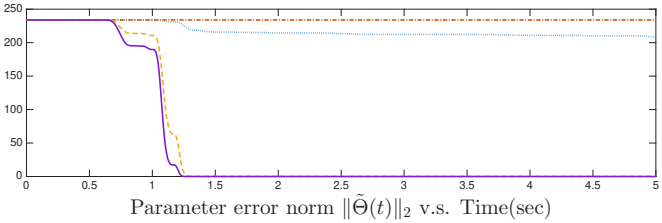

Fig. 3. Time responses of parameter estimation error norms for different cases. Case I - (red) dash-dotted line, Case II - (blue) dotted line, Case III - (yellow) dashed line and Case IV - (purple) solid line.

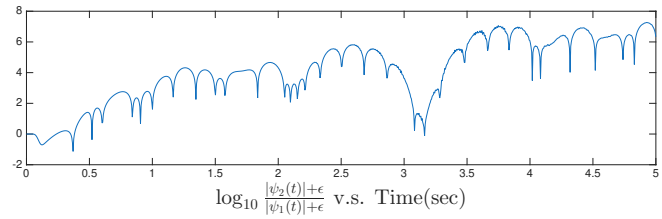

Fig. 4. Log-ratio of the magnitudes of $\psi(t)$ between the two filter sets in Cases I–IV, where $\psi_1(t)$ corresponds to the $\psi(t)$ from Case I, $\psi_2(t)$ corresponds to the $\psi(t)$ from Cases II–IV, and $\epsilon = 10^{-9}$ is used to avoid division by zero.

observation together with (27), we conclude that Case I fails to converge because the chosen filter set does not make $\int_0^t \psi^2(\tau)\, d\tau$ sufficiently large, which is required to drive the parameter estimation error to zero.

By comparing the responses of Cases II–IV, we observe that both the convergence ability and the convergence speed are influenced by the gain matrix Γ. As Γ increases, parameter error convergence can be achieved, and further increases in Γ lead to faster convergence. This observation is also consistent with the theoretical condition for parameter error convergence given in (27).

Through Cases I–IV, we examine the effects of two filter sets and three choices of the gain matrix Γ on the parameter error convergence. All simulation results across Cases I–IV are consistent with the theoretical analysis of parameter error convergence presented in (27).

In Fig. 1, we compared the torque bounds obtained from the nominal parameter values with those computed from the estimated parameters using our proposed parameter estimation scheme. The resulting curves versus speed overlap, highlighting that the bounds derived from both nominal and estimated values are consistent, which demonstrates the effectiveness of the proposed parameter estimation based torque capacity modeling method.

A comparison study. We also tested the normalized gradient adaptive algorithm for estimating the unknown parameters $\mathbf{\Theta}^*$. In this case, only one filter is required to obtain the necessary signal measurements. Thus, the adaptive law for the parameter estimate is

$$\dot{\Theta}(t) = -\Gamma_g M_g(t) N_g^{-1}(t) \left(M_g^\top(t)\hat{\Theta}(t) - Y_g(t) \right), \tag{29}$$

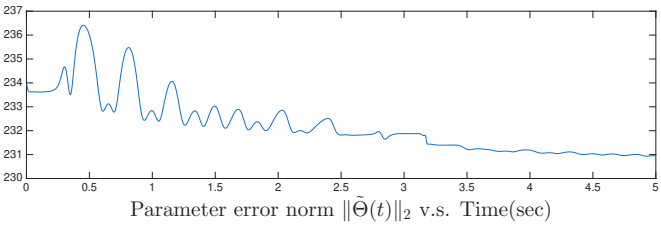

Fig. 5. Time responses of the parameter estimation error norm of the normalized gradient adaptive algorithm without DREM.

where $N_g(t) = \kappa I + M_g^\top(t) M_g(t)$, and

$$\boldsymbol{Y_g}(t) = \begin{bmatrix} \frac{1}{\Lambda_1(s)}[\mathcal{Y}_1](t) \\ \frac{1}{\Lambda_1(s)}[\mathcal{Y}_2](t) \end{bmatrix}, \boldsymbol{M}_g(t) = \begin{bmatrix} \frac{1}{\Lambda_1(s)}[\phi_1^\top](t) \\ \frac{1}{\Lambda_1(s)}[\phi_2^\top](t) \end{bmatrix}^\top. \quad (30)$$

The parameters in (29) are designed as $\kappa = 0.001$ and $\Gamma_g = \mathrm{diag}(150, 30, 30, 30, 150)$.

However, as shown in Fig. 5, the parameter error does not converge to 0, indicating the necessity of DREM.

5. CONCLUSION REMARKS AND FUTURE WORK

To accurately model the IM torque capacity, this paper proposes a parameter estimation scheme based on DREM to overcome the uncertainties caused by parameter variations during motor operation. We also study the feasibility of the corresponding parameter convergence conditions for the IM systems, and simulation results further verify the effectiveness of the proposed scheme. With this accurate IM torque capacity, we are able to design a stable and computationally efficient precision position control algorithm for the load system, using the torque capacity as an input constraint. This avoids the shortcomings of conventional trajectory generation methods, which are either overly conservative and reduce yield or fail to satisfy dynamical feasibility and reduce quality.

DECLARATION OF GENERATIVE AI AND AI-ASSISTED TECHNOLOGIES IN THE WRITING PROCESS

During the preparation of this manuscript, Copilot, ChatGPT, and Gemini were consulted for assistance with editing, grammar review, and obtaining background information. All content was reviewed by the authors, and all key ideas, analyses, and conclusions originate from the authors themselves.

REFERENCES

Ansuj, S., Shokooh, F., and Schinzinger, R. (1989). Parameter estimation for induction machines based on sensitivity analysis. *IEEE Transactions on Industry Applications*, 25(6), 1035–1040. doi:10.1109/28.44239.

Aranovskiy, S., Bobtsov, A., Ortega, R., and Pyrkin, A. (2017). Performance enhancement of parameter estimators via dynamic regressor extension and mixing. *IEEE Transactions on Automatic Control*, 62(7), 3546–3550.

Hinkkanen, M. (2004). Analysis and design of full-order flux observers for sensorless induction motors. *IEEE Transactions on Industrial Electronics*, 51(5), 1033–1040.

Holtz, J. (2006). Sensorless control of induction machines—with or without signal injection? *IEEE Transactions on Industrial Electronics*, 53(1), 7–30.

Ioannou, P.A. and Sun, J. (1996). *Robust Adaptive Control*. Prentice Hall, Upper Saddle River, NJ.

Leonhard, W. (2001). *Control of Electrical Drives*. Springer, Berlin, Heidelberg, 3rd edition.

Lu, Z., Zhang, T., and Wang, Y. (2024). Torque constraint modeling and reference shaping for servo systems. *IEEE Control Systems Letters*, 8, 2637–2642.

Qu, Z., Hinkkanen, M., and Harnefors, L. (2014). Gain scheduling of a full-order observer for sensorless induction motor drives. *IEEE Transactions on Industry Applications*, 50(6), 3834–3845.

Reddy, G.B., Poddar, G., and Muni, B.P. (2022). Parameter estimation and online adaptation of rotor time constant for induction motor drive. *IEEE Transactions on Industry Applications*, 58(2), 1416–1428.

Tao, G. (2003). *Adaptive Control Design and Analysis*. John Wiley & Sons, Hoboken, NJ.

Travieso-Torres, J.C., Lee, S.S., Veliz-Tejo, A., Leiva-Silva, F., and Ricaldi-Morales, A. (2024). Self-commissioning parameter estimation algorithm for loaded induction motors. *IEEE Transactions on Industrial Electronics*, 71(11), 13890–13900. doi:10.1109/TIE.2024.3357900.

Wang, Y., Satake, A., Sano, S., and Furutani, S. (2020). Stable adaptive estimation for speed-sensorless induction motor drives: A geometric approach. In *2020 International Conference on Electrical Machines (ICEM)*, volume 1, 1232–1238.

Wu, J., Goldsmith, A., Zhou, L., Liu, D., Wang, B., and Wang, Y. (2025). A novel high-frequency injection method towards speed-sensorless drive control of induction machines over full speed range. In *2025 IEEE International Electric Machines & Drives Conference (IEMDC)*, 949–956. IEEE.

You, J., Wu, W., and Wang, Y. (2018). An adaptive luenberger observer for speed-sensorless estimation of induction machines. In *2018 Annual American Control Conference (ACC)*, 307–312.

Zaky, M.S., Metwaly, M.K., Azazi, H.Z., and Deraz, S.A. (2018). A new adaptive smo for speed estimation of sensorless induction motor drives at zero and very low frequencies. *IEEE Transactions on Industrial Electronics*, 65(9), 6901–6911.

Zerdali, E. (2018). Adaptive extended kalman filter for speed-sensorless control of induction motors. *IEEE Transactions on Energy Conversion*, 34(2), 789–800.

Zhang, Q. (2002). Adaptive observer for multiple-input-multiple-output (mimo) linear time-varying systems. *IEEE Transactions on Automatic Control*, 47(3), 525–529. doi:10.1109/9.989154.

Zhou, L. and Wang, Y. (2016). Speed sensorless state estimation for induction motors: A moving horizon approach. In *2016 American Control Conference (ACC)*, 2229–2234. IEEE.